Model Calculations of the Atmospheric Effects of Supersonic Aviation Which Were Used in the IPCC Special Report on Aviation and the Global Atmosphere

Lead Author:
Debra Weisenstein, AER, Inc., U.S.A.

Technical Support:
Karen Sage, NASA Langley Research Center, U.S.A.
Donald Brown, NASA Langley Research Center, U.S.A.

Co-Authors:
Richard S. Eckman, NASA Langley Research Center, U.S.A.
Malcolm K.W. Ko, AER, Inc., U.S.A.

Contributors:
Steven L. Baughcum, Boeing Company, U.S.A.
Martyn Chipperfield, University of Cambridge, U.K.
Michael Gauss, University of Oslo, Norway
William L. Grose, NASA Langley Research Center, U.S.A.
Robert S. Harwood, University of Edinburgh, U.K.
Ivar Isaksen, University of Oslo, Norway
Charles H. Jackman, NASA Goddard Space Flight Center, U.S.A.
Douglas E. Kinnison, Lawrence Livermore National Laboratory, U.S.A.
Giovanni Pitari, University L'Aquila, Italy
Helen Rogers, University of Cambridge, U.K.
Courtney J. Scott, AER, Inc., U.S.A.
Peter F. Vohralik, CSIRO, Australia
Vicky West, University of Edinburgh, U.K.

May 1999

Rationale

This report is intended to expand upon the IPCC Special Report on Aviation and the Global Atmosphere. It provides additional detail regarding the supersonic emission scenario calculations presented in Chapter 4—Modeling the Future Atmosphere. Due to the space limitations in that document, detailed plots and discussion for a majority of the model calculations were omitted. This document is intended to fill that gap and has been compiled for two reasons: (1) to aid those called upon to review the IPCC Special Report, and (2) to archive and document the calculations performed by nine modeling groups for up to 50 scenarios each. This document does not attempt to provide a synthesis of the modeling results or draw conclusions regarding the impact of aircraft on the atmosphere. That function is provided by the IPCC report.

The model descriptions and model results presented in this document represent the state of those models in 1997 when the calculations were performed. Because models are continually evolving and undergoing further development, these results should be considered as a historical snapshot. Please do not cite results presented herein without first obtaining permission from the group which performed the calculations.

Contents

Chapter 2

Emission Scenarios

The future fleet of High Speed Civil Transport (HSCT) aircraft employed in these scenarios is based on the technology concept aircraft developed by the U.S. National Aeronautics and Space Administration (NASA). This developing technology is aimed at a 300 passenger aircraft with a 5000 nautical mile range cruising at Mach 2.4 at 18-20 km altitudes. Three dimensional inventories of fuel consumption and emissions based on fleets of 500 and 1000 HSCT aircraft have been developed (Baughcum and Henderson, 1998). The future date at which a viable HSCT fleet will be in operation is unknown. However, we use detailed scenarios for 2015 and 2050 in order to account for displacement of subsonic aircraft by HSCTs.

The subsonic emission scenarios for 2015 and 2050 are discussed in detail in Chapter 9 of the IPCC report. The 2015 projections were developed by NASA based on forecasts of air travel demand and aircraft technology (Baughcum et al., 1998; Mortlock and van Alstyne, 1998). The "background" scenarios with 2015 boundary conditions (Scenarios D, D3-D8) use this subsonic fleet projection. The 2050 projections were developed by the International Civil Aviation Organization Forecasting and Economic Support Group (FESG) (CAEP/4-FESG/Report-4, 1998). These long range projections are much more uncertain, and therefore three different subsonic fleet scenarios have been employed for 2050 modeling. Background Scenario D9, with 2050 boundary conditions, employs the NASA 2015 fleet projection. Scenario F employs the FESG base case projections to 2050 based on IPCC GDP Scenario IS92a, and Scenario G employs the 2050 FESG high demand projections based on IPCC GDP Scenario IS92e. Technology Scenario 1 is employed in both cases for converting passenger-kilometers to emissions.

2.1 Fuel Use

Fuel use inventories were compiled for the projected fleets as functions of latitude, longitude, and altitude on a 1^ox1^ox1 km pressure altitude grid. Seasonal variations in fleet utilization and emissions were not considered. Figure 2.1 shows vertically-integrated fuel use from the projected 2015 subsonic fleet as a function of latitude and longitude. Figures 2.2 and 2.3 show similar plots for the projected 2050 fleets under the IS92a and high demand IS92e assumptions, respectively. The flight tracks of the projected HSCT aircraft fleet are evident in Figure 2.4, which shows fuel use above 13 km by the 500 HSCT fleet. HSCT aircraft are expected to be used for intercontinental and long-distance routes primarily over water, due to the need to minimize sonic booms over populated land masses. Fuel use above 13 km by the 1000 aircraft HSCT fleet is shown in Figure 2.5 as a function of latitude and longitude. The projected 1000 HSCT fleet is not a scaled version of the 500 HSCT fleet, but a separate projection which includes a greater percentage of flights in Asia.

The HSCT scenarios, which include an "S" in the scenario descriptor, include both a subsonic and a supersonic fleet. The subsonic fleet has been reduced relative to the subsonic-only scenarios to account for passenger demand displacement from subsonic to supersonic aircraft. Fuel use by both subsonic and supersonic aircraft is shown in Figure 2.6 for the 500 aircraft HSCT fleet together with the adjusted 2015 subsonic fleet as a function of latitude and altitude. Figure 2.7 shows a similar plot for the 1000 HSCT scenario. Fuel use integrated over latitude and longitude, ie. as a function of altitude only, is shown in Figure 2.8 The 2015 subsonic only fleet, the 500 HSCT fleet, and the 1000 HSCT fleet are shown by separate bars in the histogram. Notice that the 1000 HSCT fleet at cruise altitude does not consume twice the fuel of the 500 HSCT fleet, but only 80% more (see Baughcum and Henderson, 1995). A histogram of the vertical distribution of fuel use in 2050 for the 1000 HSCT fleet along with the IS92a subsonic scenario is shown in Figure 2.9. Figure 2.10 show a similar histogram plot using the 2050 IS92e high demand subsonic fleet. A summary of fuel use for the included scenarios is given in Table 2.1, showing total fuel use and fuel use above and below 13 km.

Table 2.1: Fuel Use Projected for the Future Aircraft Scenarios

Scenario	Total Fuel (Tg/yr)	Fuel Burned below 13 km (Tg/yr)†	Fuel Burned above 13 km (Tg/yr)
2015 Subsonic	309	307	2
2015 Subsonic + 500 HSCTs	338	282	56
2015 Subsonic + 1000 HSCTs	378	279	99
2050 Subsonic IS92a	471	469	2
2050 Subsonic IS92a + 1000 HSCTs	557	458	99
2050 Subsonic IS92e High Demand	744	742	2
2050 Subsonic IS92e + 1000 HSCTs	831	732	99

†Note that scenarios which include supersonic aircraft use a reduced subsonic fleet to account for a shift in passenger demand.

2.2 HSCT Emissions

Because the HSCT technology is still in the research and development stage, operating parameters and emission indices (EI, grams of pollutant emitted per kilogram of fuel burned) are quite uncertain, and are therefore treated parametrically in this study. Aircraft emissions of H_2O, NO_x, and sulfur are the most significant to atmospheric ozone response. Emissions of CO and hydrocarbons were included in the atmospheric modeling performed for IPCC, but their emissions do not constitute a large perturbation to their background concentrations and thus do not influence ozone to a significant extent. Emissions of CO_2 do not chemically interact with ozone. CO_2 may impact ozone indirectly by modifying atmospheric temperature and circulation, but this effect is not accounted for by most of the models used here. Emission of soot particles is also ignored.

Table 2.2 lists the pollutants considered in the current modeling study and their emissions above 13 km. Emission indices (in grams of pollutant per kg fuel burned) for the aircraft at cruise are also shown. H_2O emissions are strictly proportional to fuel use, with an $EI(H_2O)=1230$. The NO_x emission indices are given as grams NO_2 equivalent per kg fuel burned and are treated parametrically. Projected emission indices for CO are 2.9 and for hydrocarbons 0.3. Most models represent all the hydrocarbon emissions as CH_4, even though aircraft are known to emit a variety of hydrocarbons. Sulfur (SO_x) emissions are not included in many of the emission scenarios. Where they are included, an $EI(SO_x)$ of 0.4 gm SO_2 per kg fuel burned is employed, which represents a 50% reduction in fuel sulfur content from the current world average. Total emissions are projected on an annual basis. The models treat this emission as a continuous input flux at a fixed rate in molecules per second per grid box volume.

The NASA technology program is aggressively pursuing a combustor with an $EI(NO_x)$ of 5. However, the emission scenarios treat this parameter parametrically and consider three values of $EI(NO_x)$: 5, 10, and 15. The subsonic fleet projection accounts for different values of $EI(NO_x)$ for different engine types and operating conditions and yields a weighted average $EI(NO_x)$ of approximately 13 gm/(kg fuel). Vertical profiles of NO_x emissions, integrated over latitude and longitude, are shown in Figure 2.11 with $EI(NO_x)$ of 5 for the HSCT aircraft. The 2015 subsonic only fleet, the 500 HSCT fleet, and the 1000 HSCT fleet are shown by separate bars in the histogram.

Table 2.2: Emissions by Projected HSCT Fleets above 13 km

Pollutant	Emission Index	500 HSCT Fleet (Gg/yr)	1000 HSCT Fleet (Gg/yr)
H_2O	1230	66,300	119,400
NO_x	$5^\dagger$	269	486
	$10^\dagger$	539	971
	$15^\dagger$	808	1460
CO	2.9	155	279
Hydrocarbons	$0.3^\ddagger$	15.7	28.2
SO_x	0	0	0
	$0.4^\sharp$	21.6	38.8

$^\dagger NO_x$ emission index given as NO_2 equivalent.
‡Hydrocarbon emission index given as CH_4 equivalent.
$^\sharp SO_x$ emission index given as SO_2 equivalent.

2.3 Sulfur Emission Scenarios

Sulfur emissions are a large uncertainty in the present assessment of the impact of aircraft on the atmosphere. The total emission of sulfur from aircraft depends on the sulfur content of the fuel. Sulfur content varies widely in current fuels. Economic or environmental considerations may lead to reductions in sulfur in future fuel supplies. Among the scenarios considered for this report, most omit sulfur emissions, equivalent to assuming desulfurized fuel. Others assume an EI(SO_x) of 0.4 grams SO_2/(kg fuel) as a sensitivity study of the effects of sulfur from aircraft on atmospheric ozone. The EI(SO_x) averaged over the current subsonic fleet is about 0.8.

The fractionation of emitted sulfur species is unknown, but may include SO_3 and H_2SO_4 in addition to SO_2. The SO_3 and H_2SO_4 are expected to form sulfuric acid aerosol particles within the near-field aircraft plume. Such particles have been observed (Fahey et al., 1995; Miake-Lye et al., 1998; Anderson et al., 1998; Hagen et al., 1998) The fraction of sulfur converted to particles within the aircraft plume may be a complex function of engine type, operating parameters, fuel sulfur content, and ambient conditions. Previous studies (Weisenstein et al., 1996; Weisenstein et al., 1998) have found large sensitivities in both global sulfate aerosol surface area density (SAD) and ozone response to the assumed particle conversion fraction. Therefore this parameter is treated parametrically, with values of 0%, 10%, 50%, and 100% employed. The number of particles emitted and their size distribution are less important, as coagulation within the plume will tend to reduce the number density and increase the average diameter during plume evolution.

Because most models participating in this study did not have the capability to handle sulfur emission and calculate perturbations to sulfate aerosol, the sulfate surface area density (SAD) was specified as a scenario input. Microphysical calculations were performed by the AER 2-D model (Weisenstein et al., 1997) to calculate the SAD perturbation due to a given sulfur emission scenario. Sulfate particles formed in the plume were assumed to be 10 nm in radius. Only sulfur emissions above 13 km were used in the calculations to avoid increasing the number of subsonic scenarios and due to the greater uncertainty involved in modeling tropospheric sulfur. The calculated perturbations were added to the SA0 volcanically clean surface area density defined in WMO (1992). SAD fields were kept constant from January to June and from July to December, in accordance with the definition of SA0. Scenario definitions are presented in Table 2.3, which also includes the percent change in calculated SAD relative to the SA0 background surface area distribution in the 14-21 km, 33-90^{o}N region. Figures 2.12-2.16 shows the zonal mean SAD perturbations used by all modelers for those scenarios which include aircraft sulfur emissions.

Table 2.3: Sulfate Surface Area Density (SAD) Scenario Definitions for Various HSCT Emission Assumptions

SAD Name	HSCT Fleet Size	Cruise Altitude	SO_2 Gas to Particle Conversion	Change in SAD[†] (14-21 km, 33-90^{o}N)	Reference
SA0[‡]	-	-	-		WMO (1992)
SA1	500	Std	50%	82%	AER 2-D Model
SA2	1000	Std	50%	124%	AER 2-D Model
SA2-2km	1000	-2km	50%	57%	AER 2-D Model
SA3	500	Std	100%	111%	AER 2-D Model
SA4	1000	Std	100%	164%	AER 2-D Model
SA5	500	Std	10%	38%	AER 2-D Model
SA6	1000	Std	10%	74%	AER 2-D Model
SA6-2km	1000	-2km	10%	22%	AER 2-D Model
SA7	500	Std	0%	26%	AER 2-D Model

[†]Percent change is relative to SA0.
[‡]SA0 represents the volcanically clean background sulfate aerosol distribution without aircraft influence.

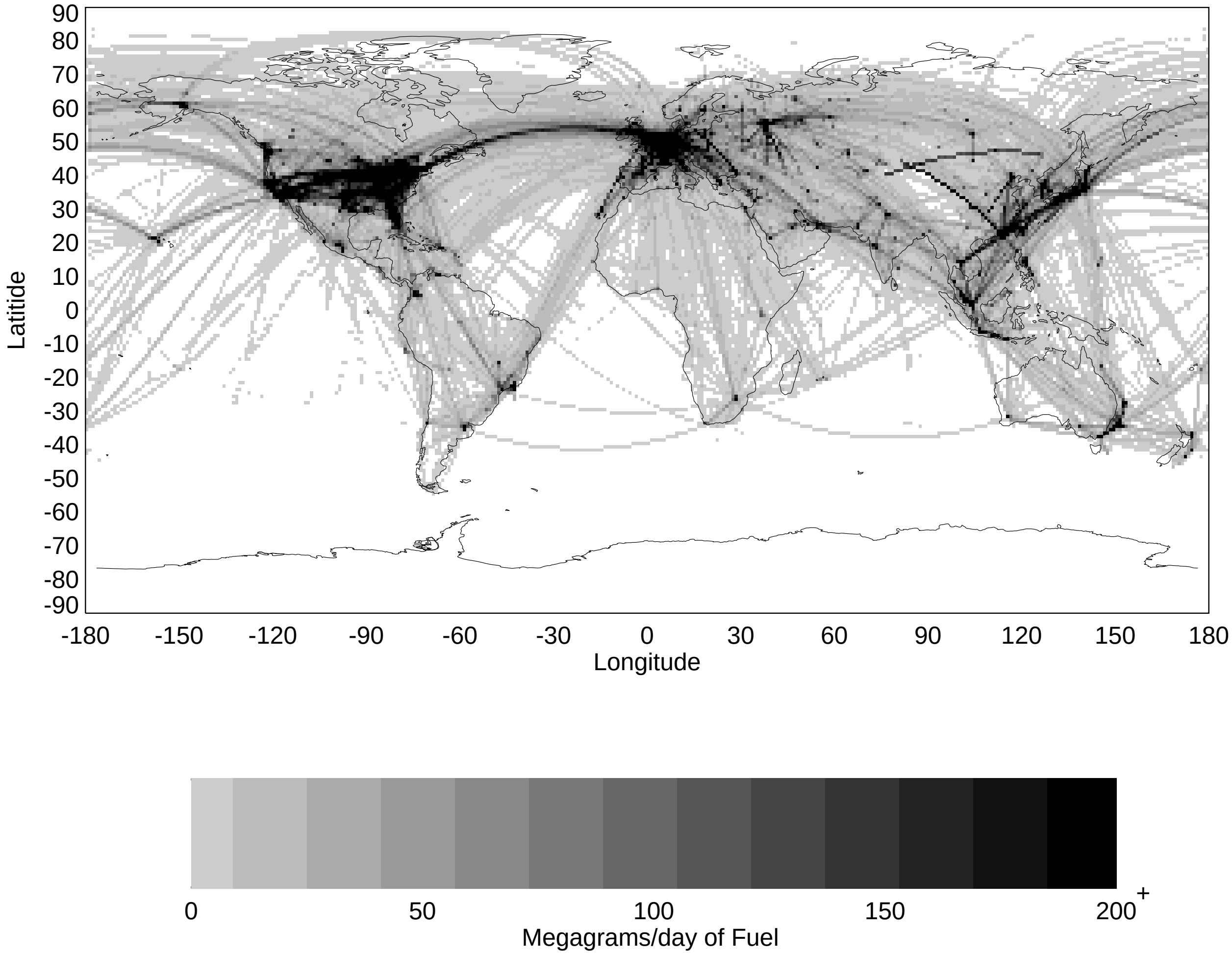

Figure 2.1: Total fuel use for the projected 2015 subsonic fleet according to the NASA emission scenario as a function of latitude and longitude.

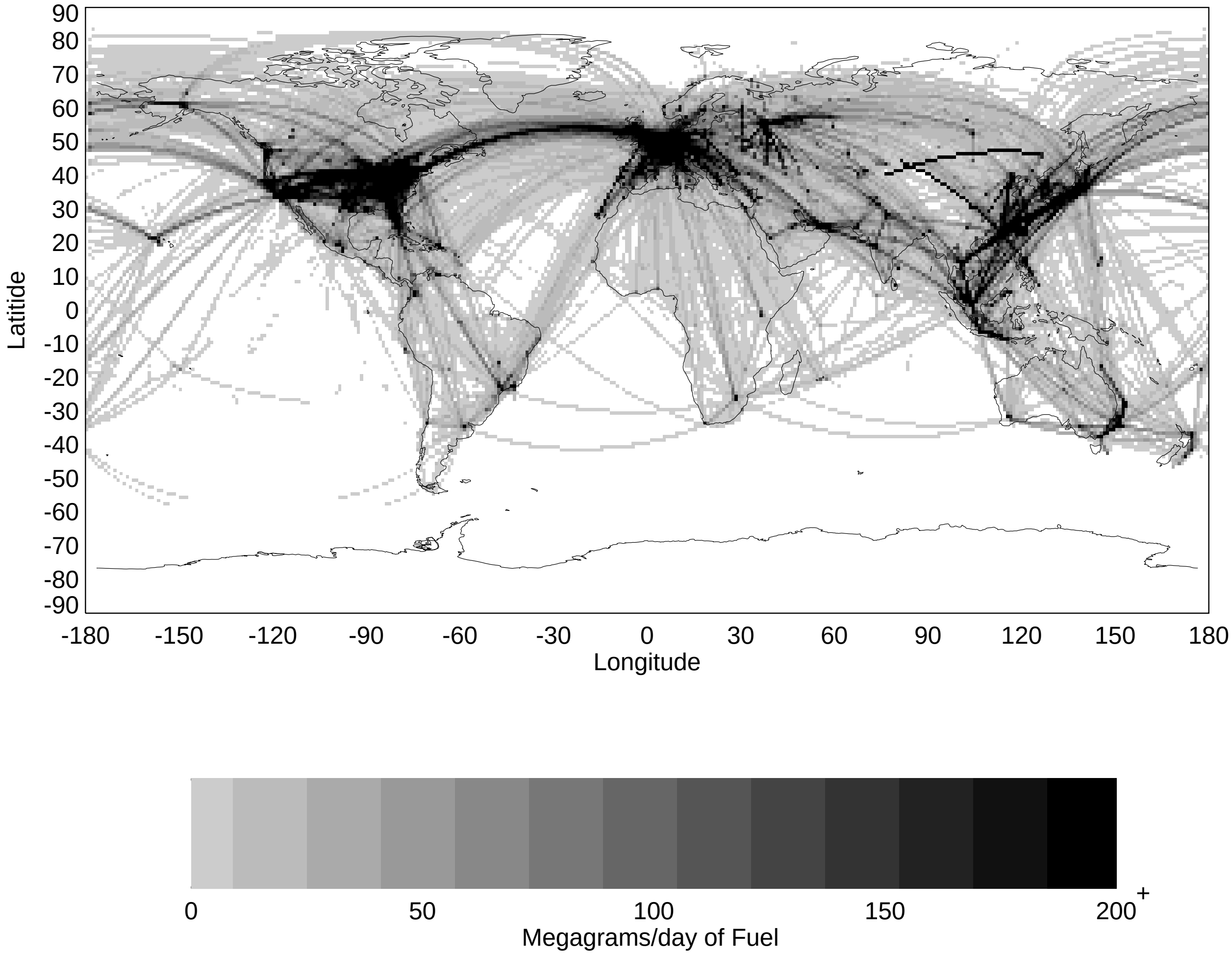

Figure 2.2: Total fuel use for the projected 2050 subsonic fleet according to the FESG IS92a scenario as a function of latitude and longitude.

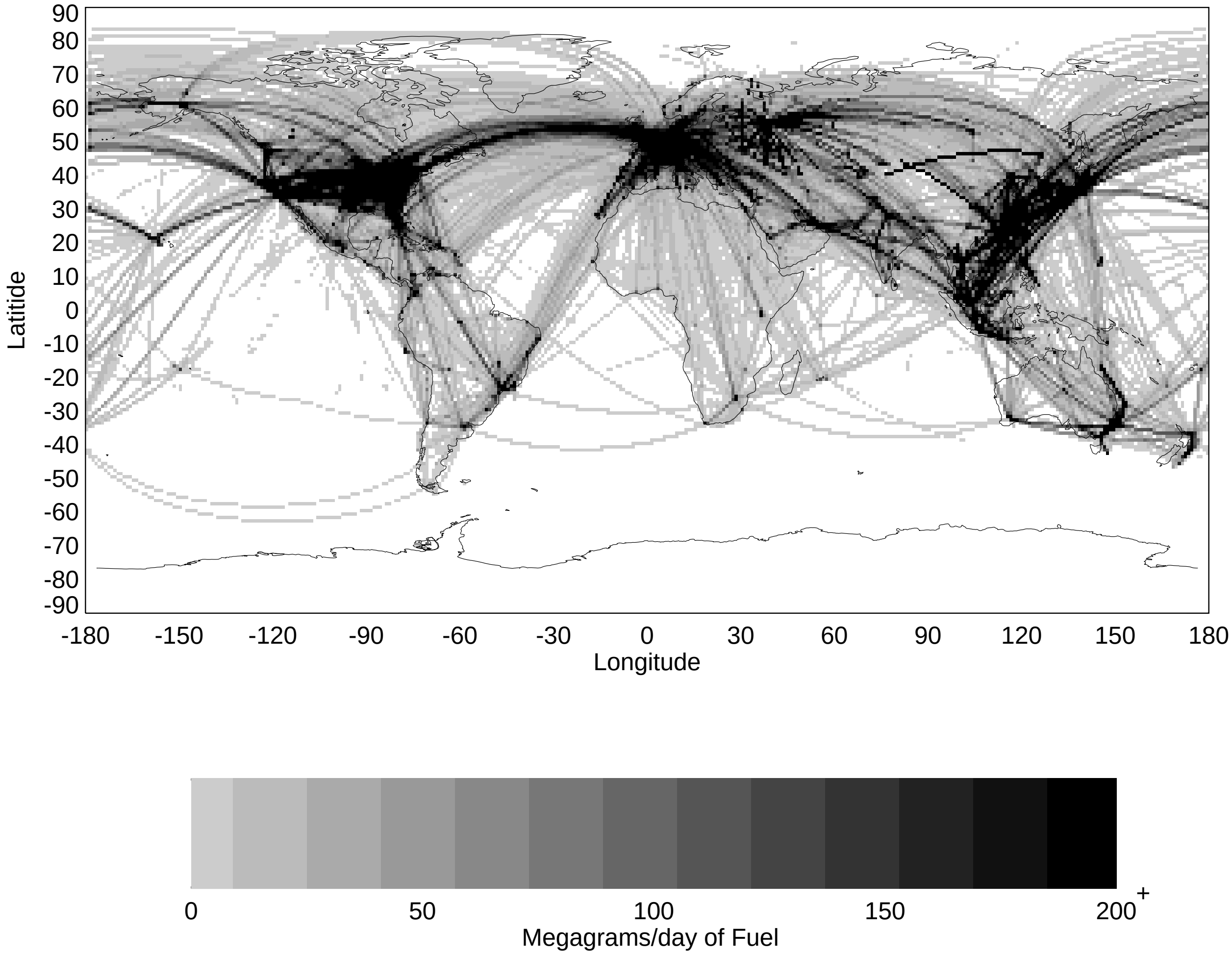

Figure 2.3: Total fuel use for the projected 2050 subsonic fleet according to the FESG IS92e high demand scenario as a function of latitude and longitude.

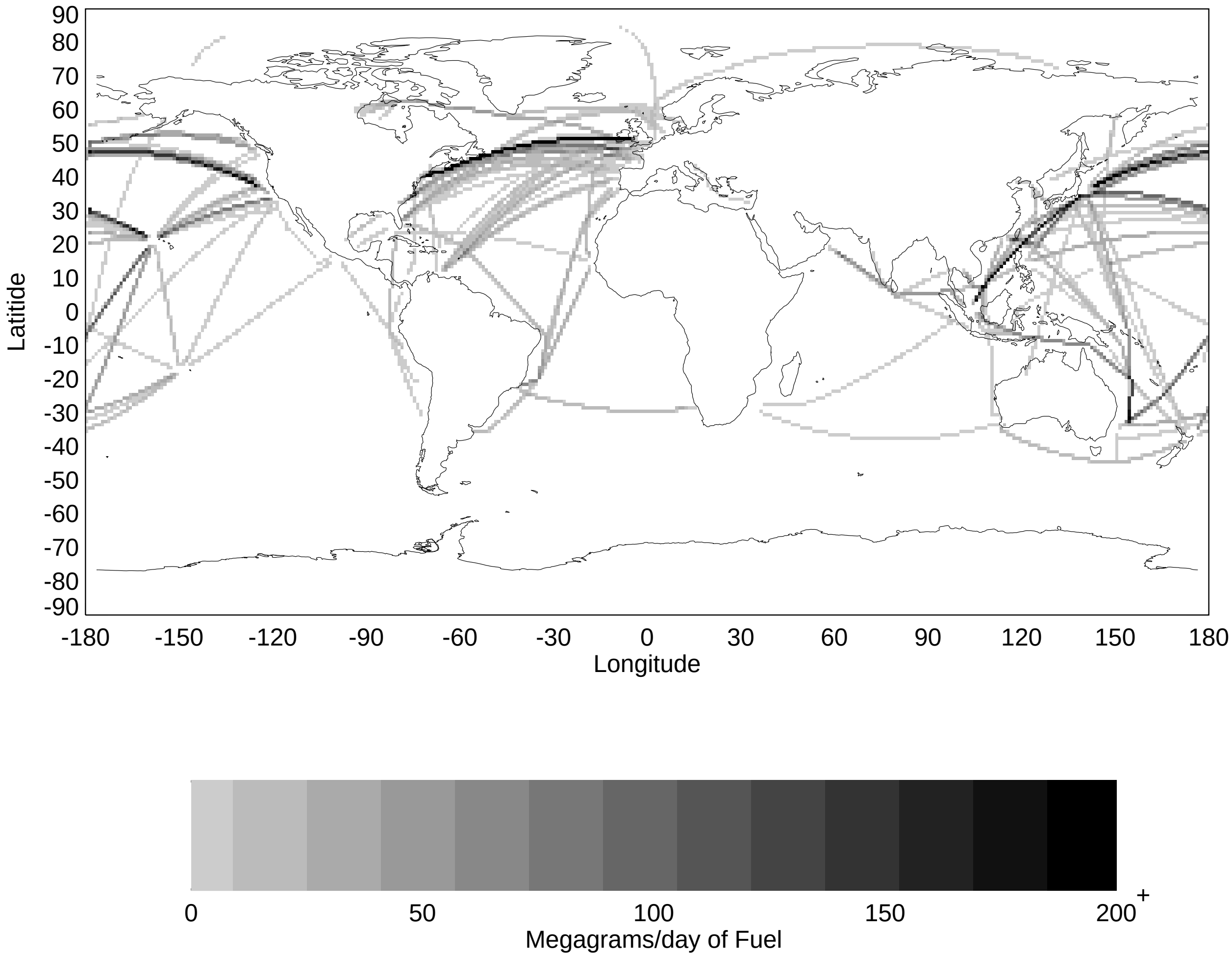

Figure 2.4: Fuel use above 13 km for the projected fleet of 500 HSCTs as a function of latitude and longitude.

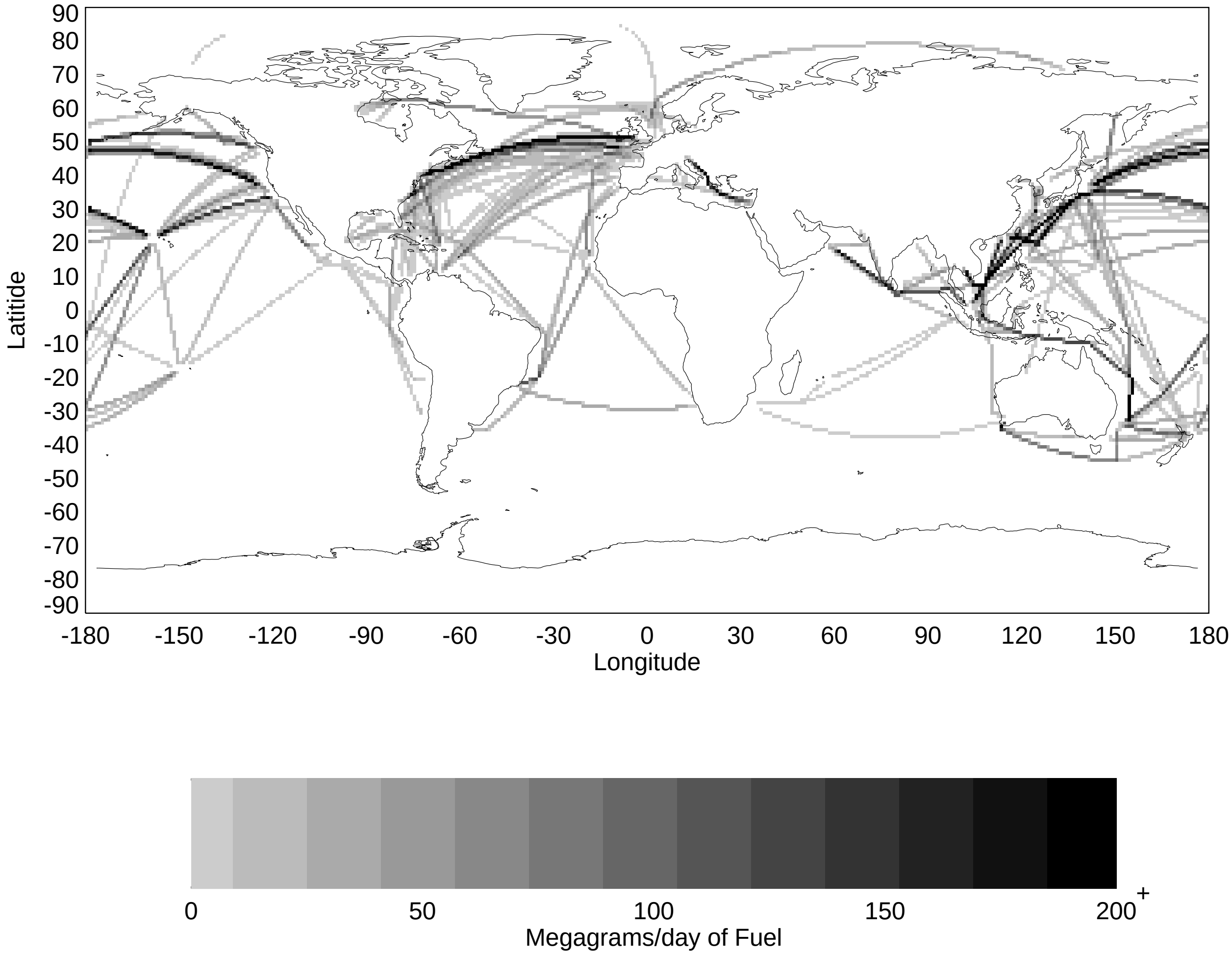

Figure 2.5: Fuel use above 13 km for the projected fleet of 1000 HSCTs as a function of latitude and longitude.

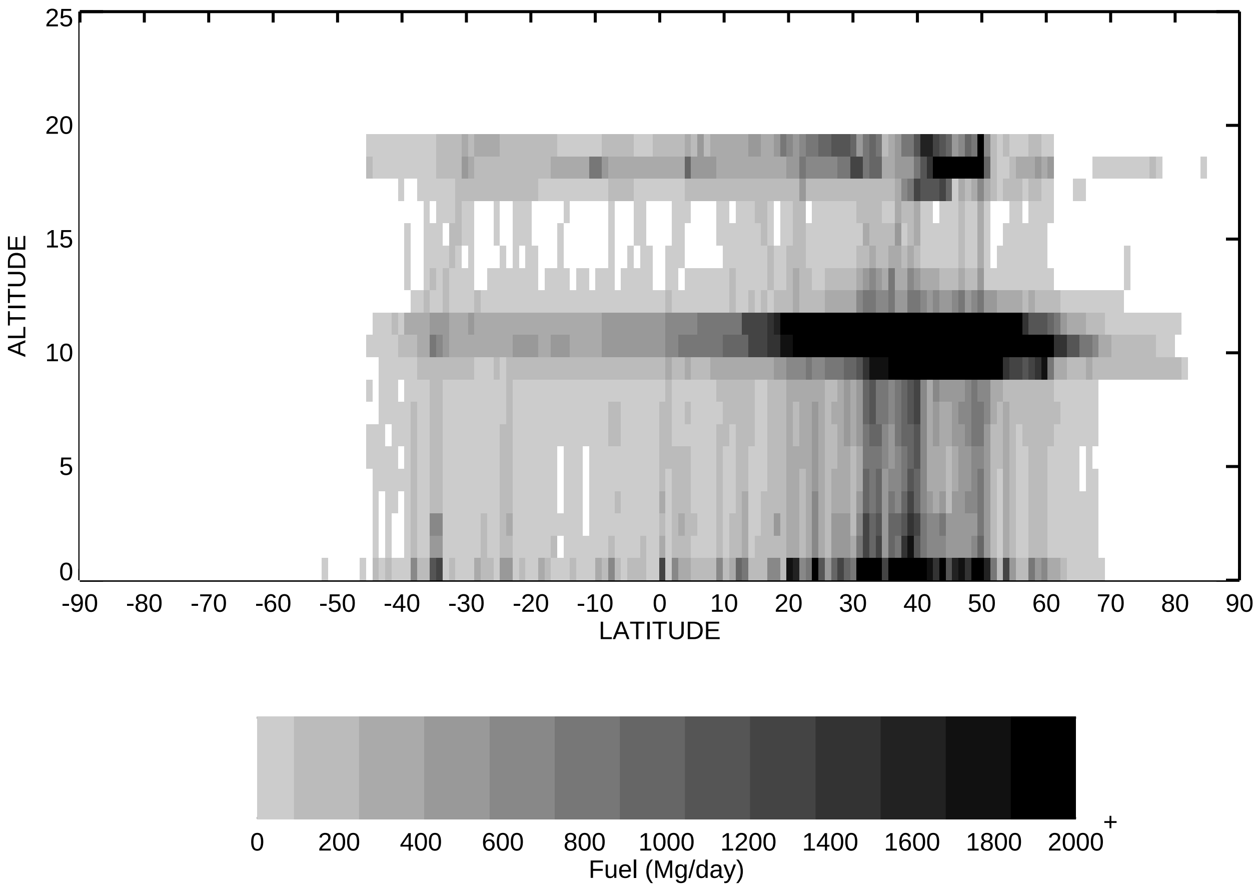

Figure 2.6: Total fuel use for the projected 500 HSCT fleet combined with the 2015 subsonic fleet as a function of latitude and altitude.

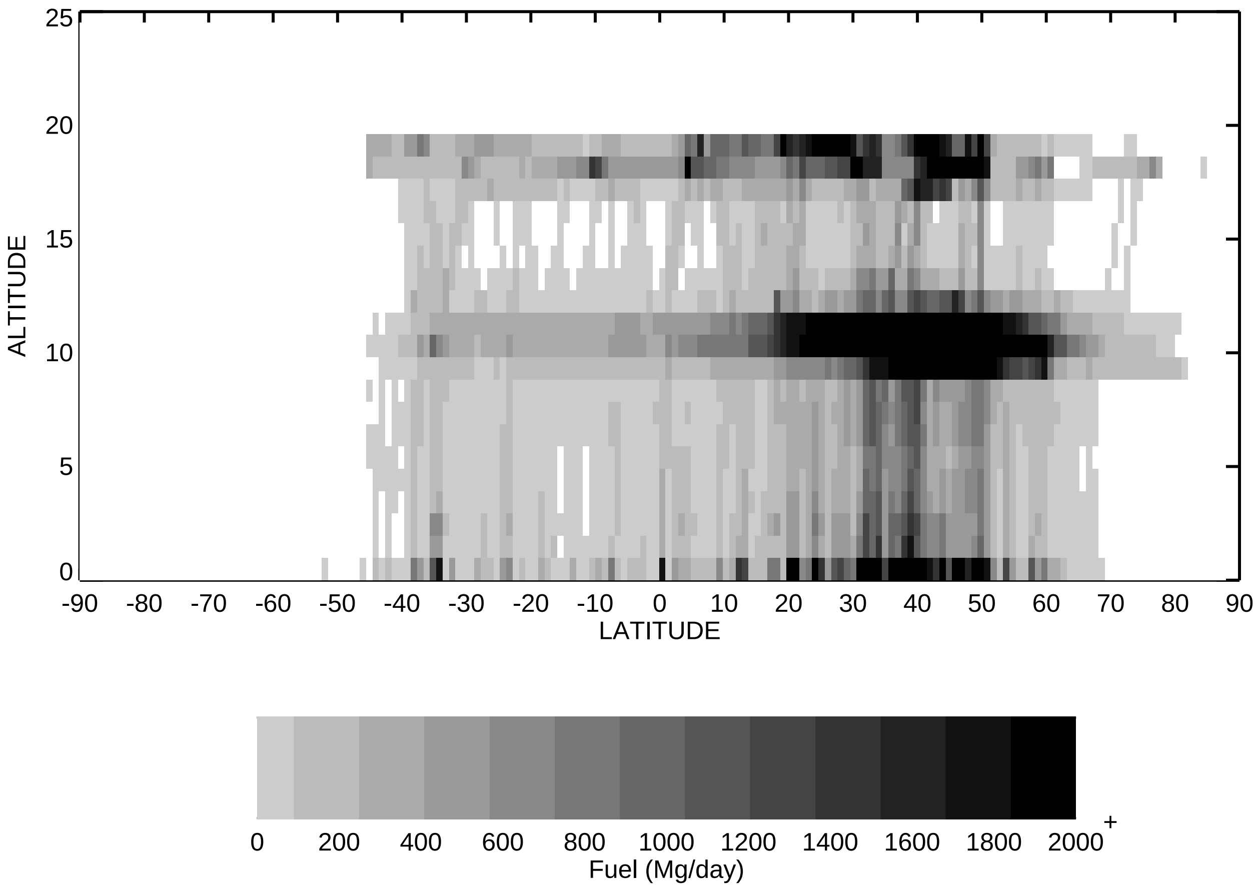

Figure 2.7: Total fuel use for the projected 1000 HSCT fleet combined with the 2015 subsonic fleet as a function of latitude and altitude.

Figure 2.8: Total fuel use as a function of altitude for the projected 500 and 1000 HSCT scenarios along with the 2015 subsonic-only scenario.

Figure 2.9: Total fuel use as a function of altitude for the projected 1000 HSCT scenario along with the 2050 IS92a subsonic-only scenario.

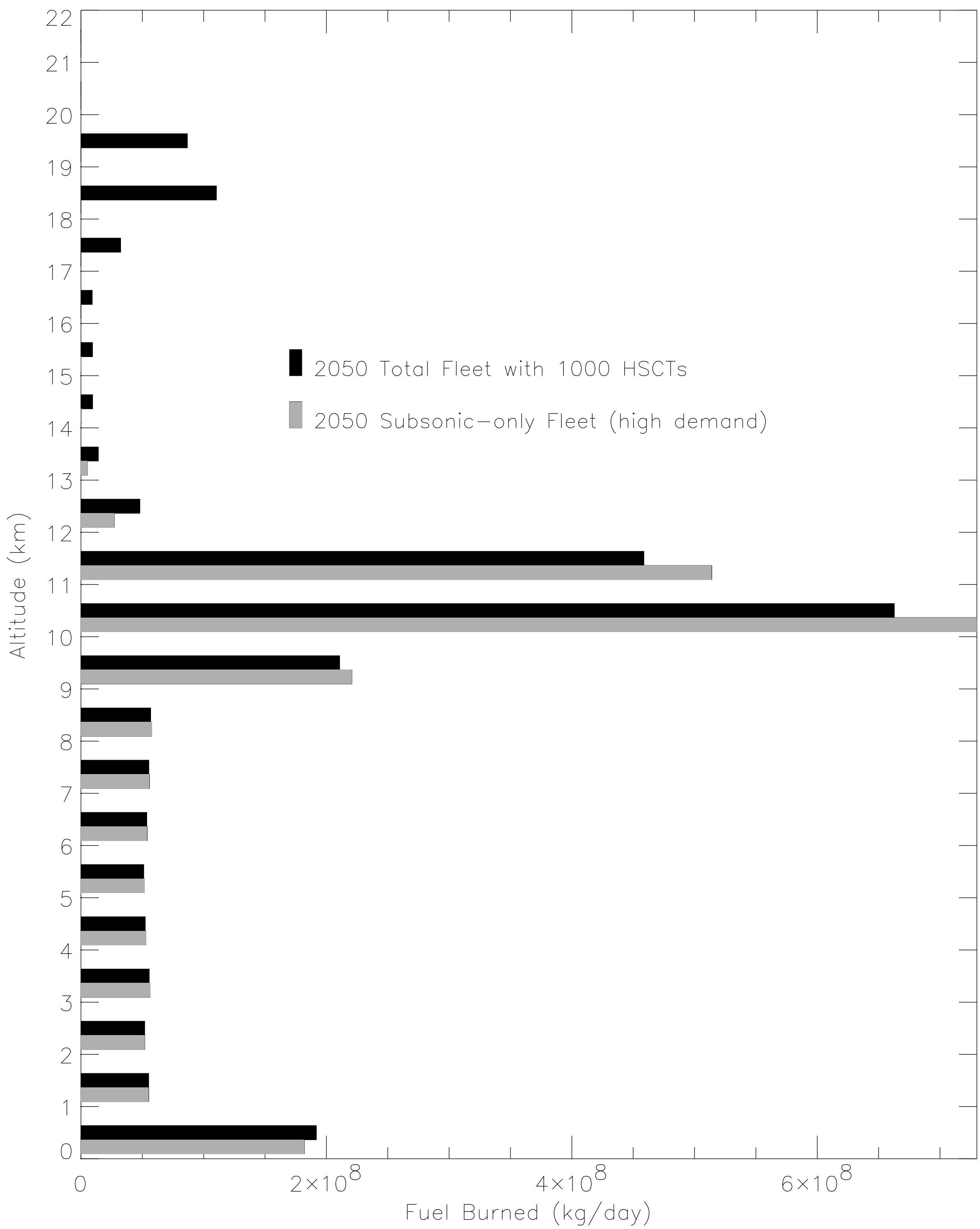

Figure 2.10: Total fuel use as a function of altitude for the projected 1000 HSCT scenario along with the 2050 IS92e high demand subsonic-only scenario.

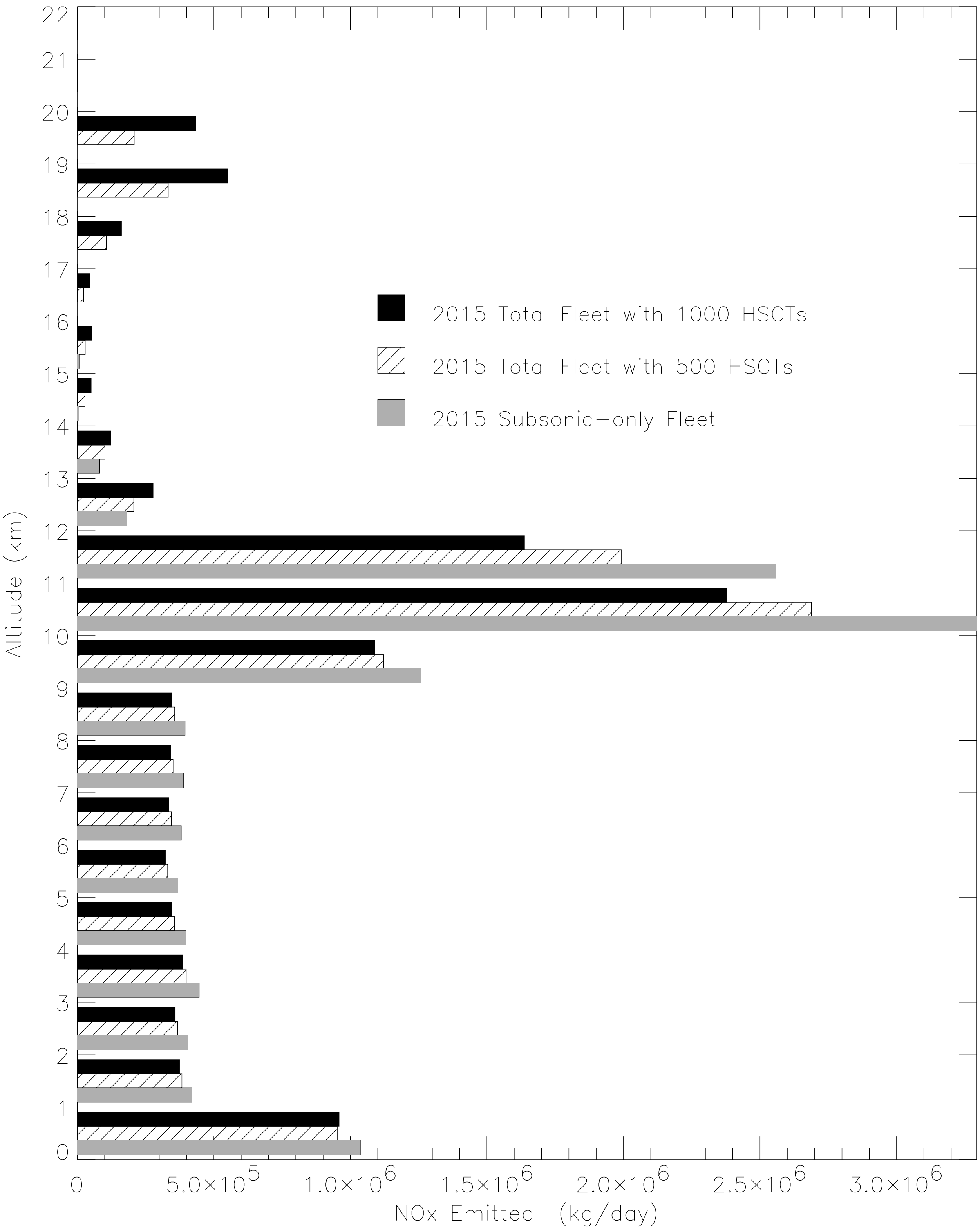

Figure 2.11: NO_x emissions for $EI(NO_x)$=5 as a function of altitude for the projected 500 and 1000 HSCT scenarios along with the 2015 subsonic-only scenario. .

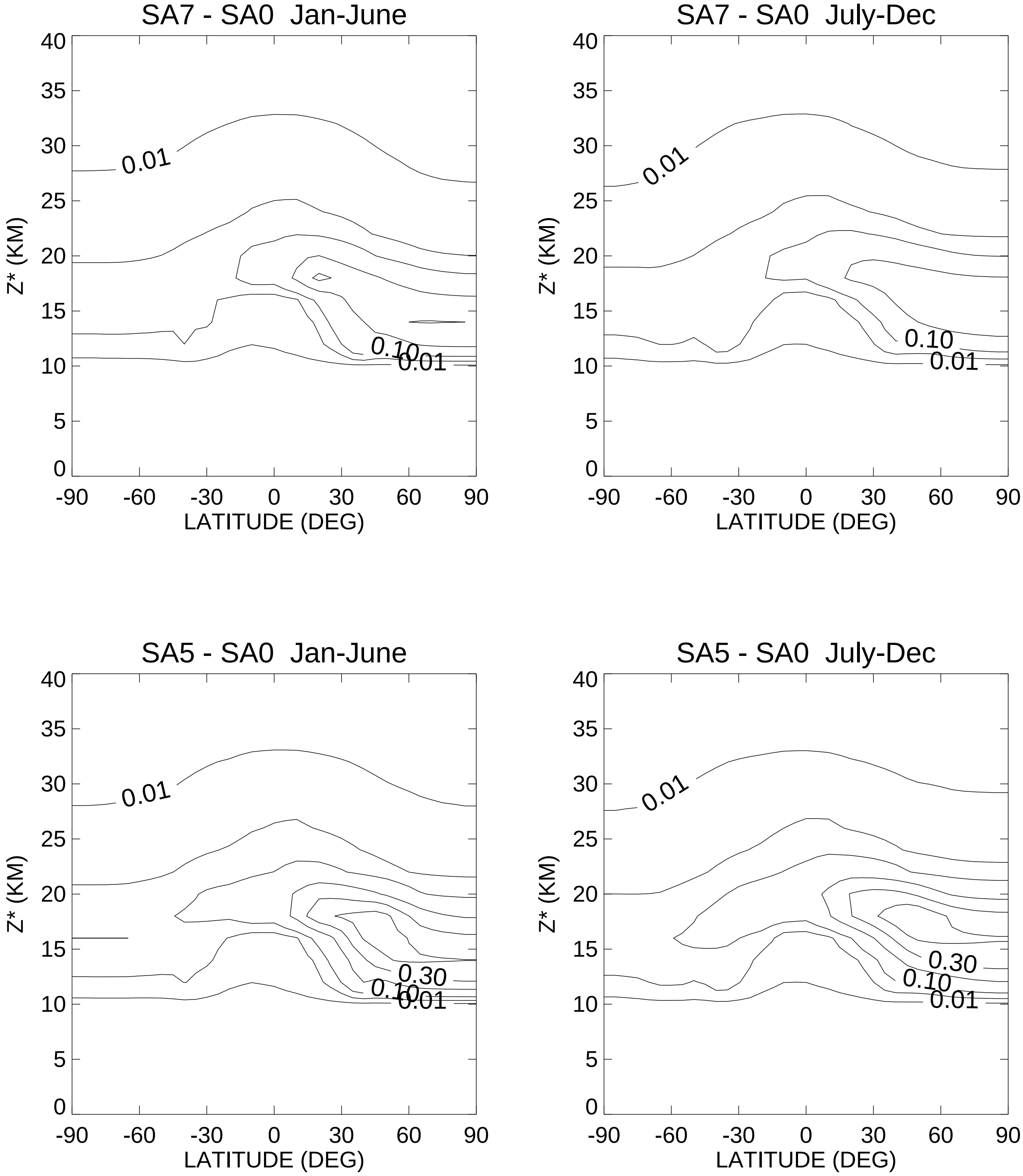

Figure 2.12: Aerosol surface area density ($\mu m^2/cm^3$) perturbations relative to SA0 as calculated by the AER 2-D sulfate aerosol model. These scenarios represent sulfur emissions from 500 HSCTs with EI(SO_2)=0.4 and 0% (for SA7) or 10% (for SA5) gas to particle conversion in the plume. Contour levels are 0.01, 0.05, 0.1, 0.2, 0.3, 0.4.

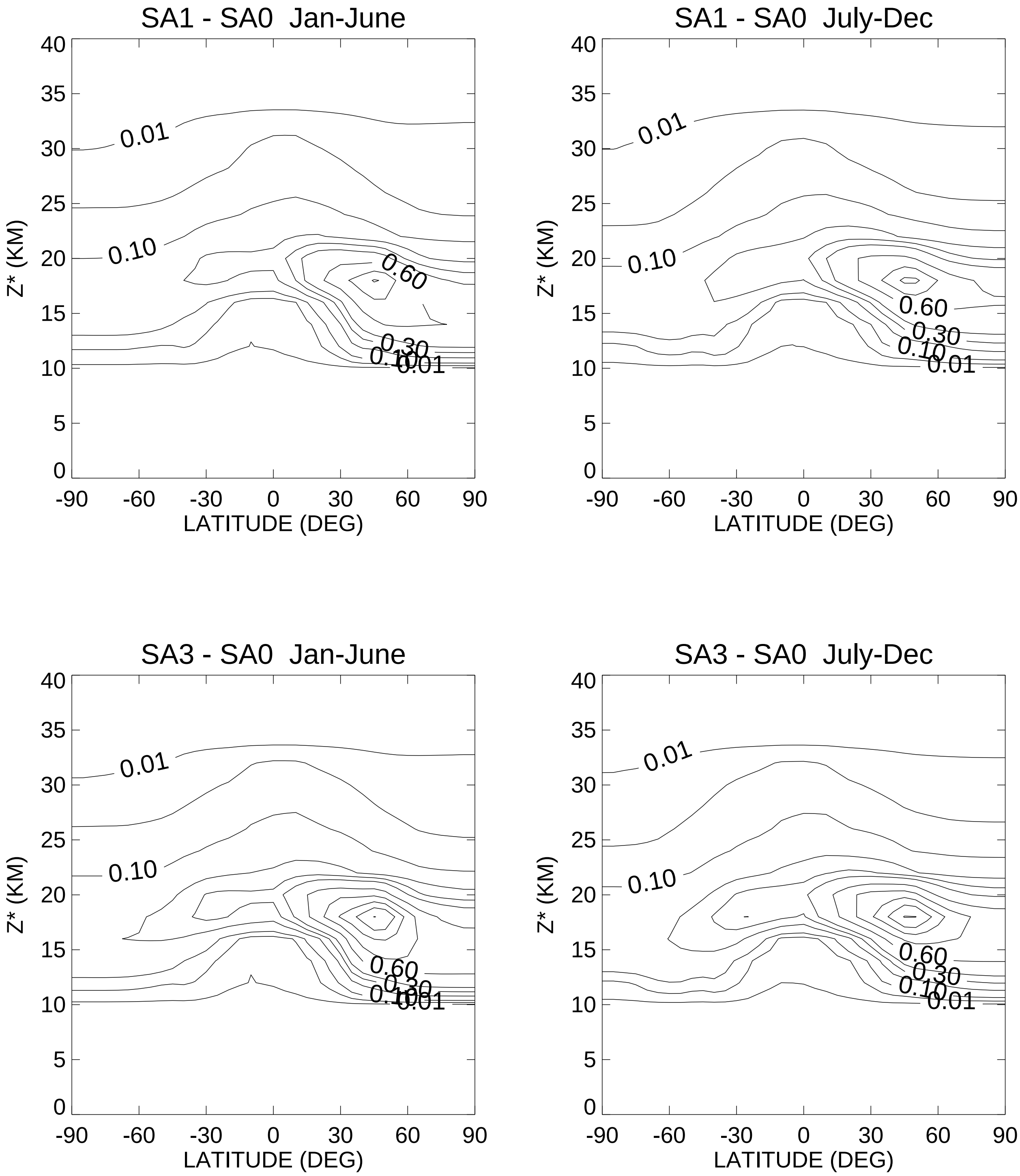

Figure 2.13: Aerosol surface area density ($\mu m^2/cm^3$) perturbations relative to SA0 as calculated by the AER 2-D sulfate aerosol model. These scenarios represent sulfur emissions from 500 HSCT with EI(SO_2)=0.4 and 50% (for SA1) or 100% (for SA3) gas to particle conversion in the plume. Contour levels are 0.01, 0.05, 0.1, 0.2, 0.3, 0.4, 0.6, 0.8, 1.0, 1.2, 1.5.

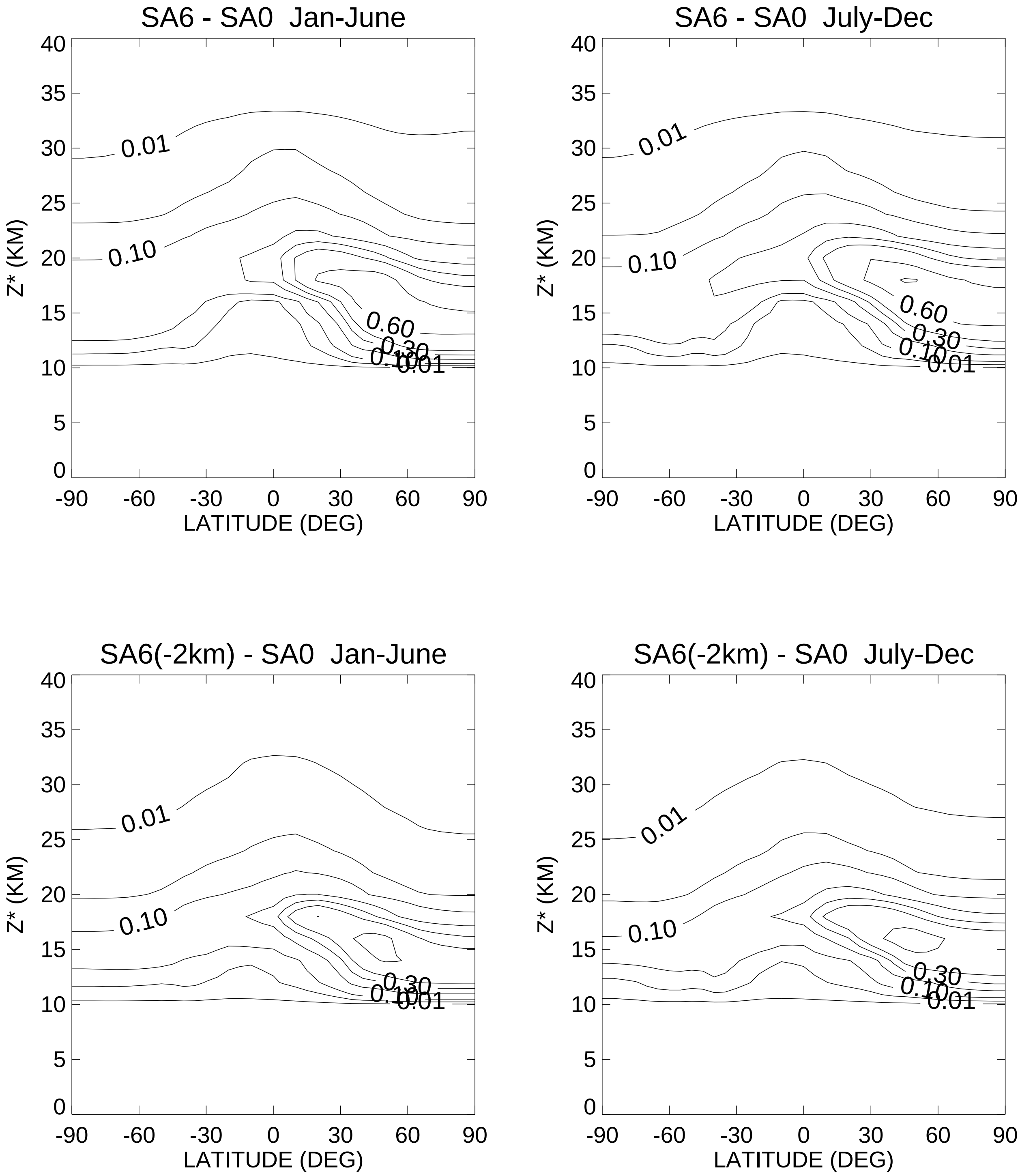

Figure 2.14: Aerosol surface area density ($\mu m^2/cm^3$) perturbations relative to SA0 as calculated by the AER 2-D sulfate aerosol model. These scenarios represent sulfur emissions from 1000 HSCT with EI(SO_2)=0.4 and 10% gas to particle conversion in the plume and standard cruise altitude (SA6) or cruise altitude decreased by 2 km (SA6-2km). Contour levels are 0.01, 0.05, 0.1, 0.2, 0.3, 0.4, 0.6, 0.8.

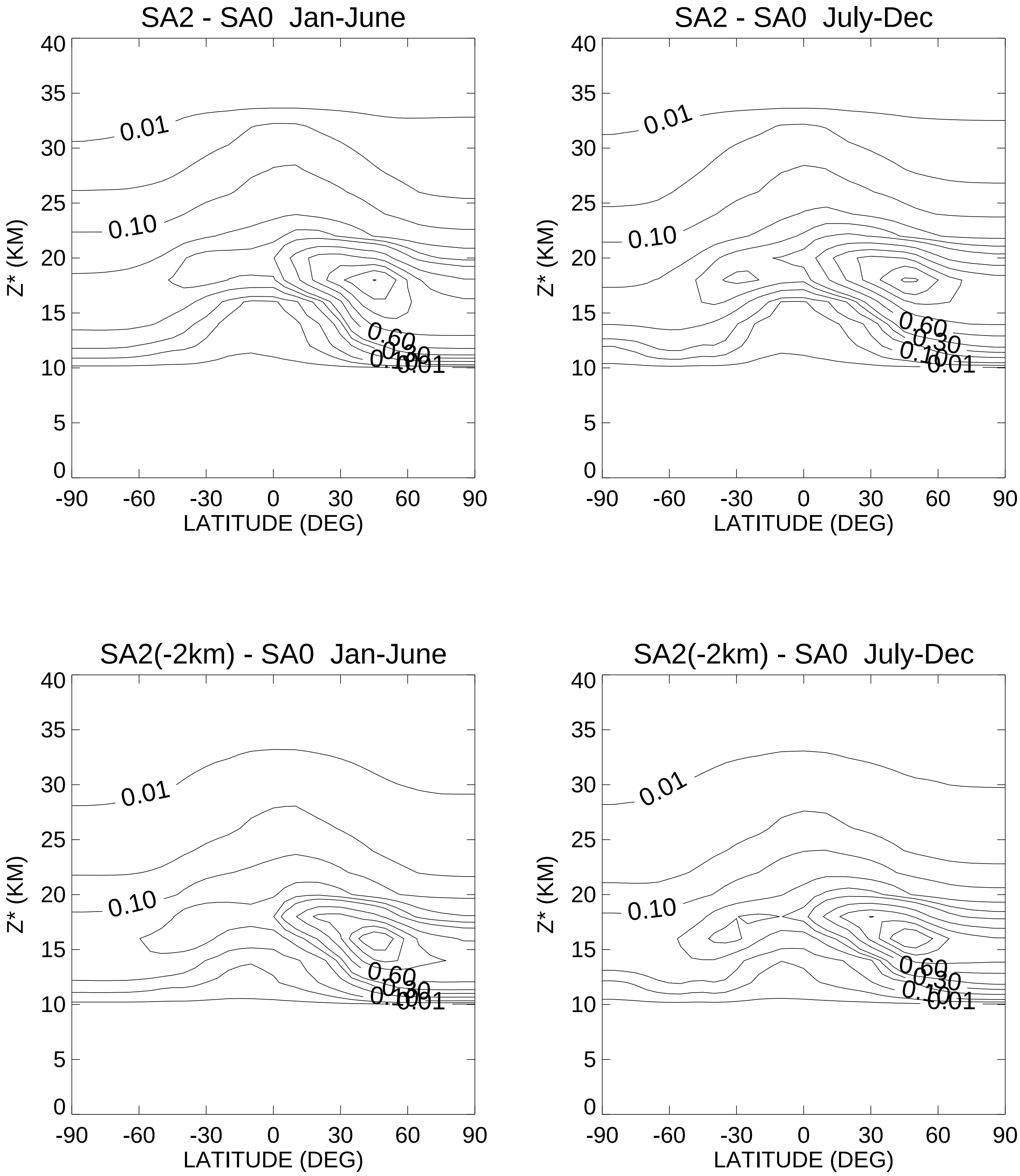

Figure 2.15: Aerosol surface area density ($\mu m^2/cm^3$) perturbations relative to SA0 as calculated by the AER 2-D sulfate aerosol model. These scenarios represent sulfur emissions from 1000 HSCT with EI(SO_2)=0.4 and 50% gas to particle conversion in the plume and standard cruise altitude (SA2) or cruise altitude decreased by 2 km (SA2-2km). Contour levels are 0.01, 0.05, 0.1, 0.2, 0.3, 0.4, 0.6, 0.8, 1.0, 1.2, 1.5.

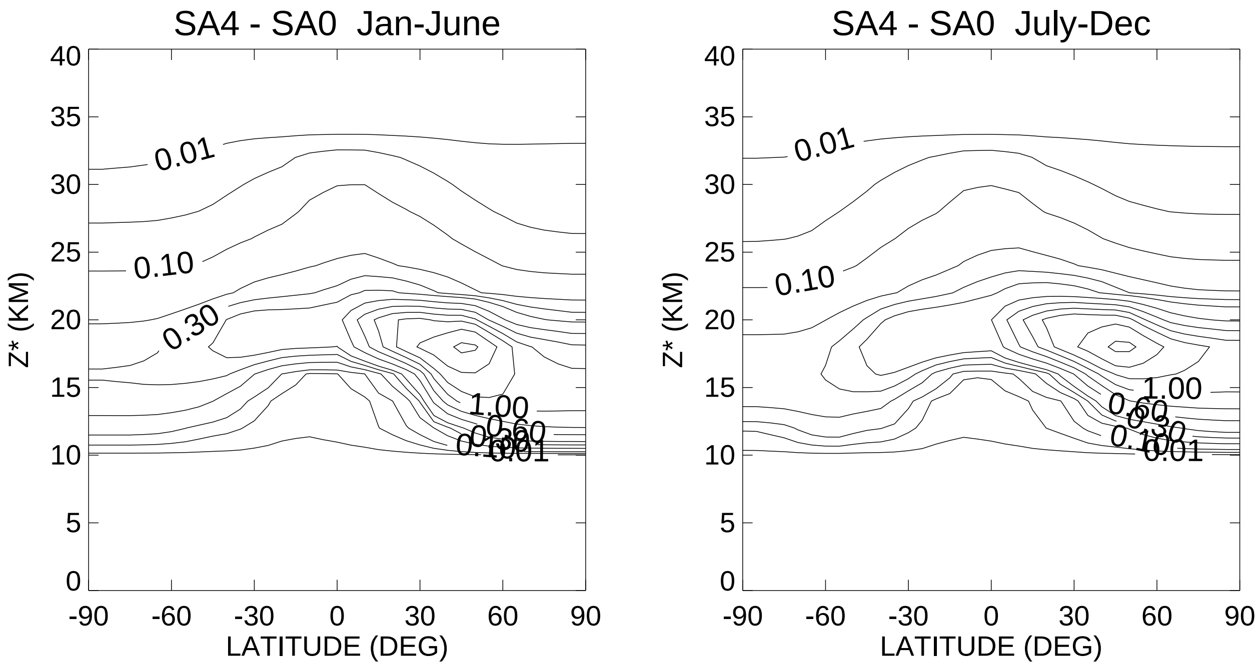

Figure 2.16: Aerosol surface area density ($\mu m^2/cm^3$) perturbations relative to SA0 as calculated by the AER 2-D sulfate aerosol model. This scenario (SA4) represents sulfur emissions from 1000 HSCTs with EI(SO_2)=0.4 and 100% gas to particle conversion in the plume. Contour levels are 0.005, 0.01, 0.05, 0.1, 0.2, 0.3, 0.4, 0.5, 1.0, 1.5, 2.0.

Bibliography

[1] Anderson, B. E., W. R. Cofer, J. D. Barrick, D. R. Bagwell, and C. H. Hudgins, Airborne observations of aircraft aerosol emissions II: Factors controlling volatile particle production, *Geophys. Res. Lett., 25,* 1693-1696, 1998.

[2] Baughcum, S. L. and S. C. Henderson, Aircraft Emission Inventories Projected in Year 2015 for a High Speed Civil Transport (HSCT) Universal Airline Network, *NASA CR-4659,* 1995.

[3] Baughcum, S. L. and S. C. Henderson, Aircraft Emission Scenarios Projected in Year 2015 for the NASA Technology Concept Aircraft (TCA) High Speed Civil Transport, *NASA CR-1998-207635,* 1998.

[4] Baughcum, S. L., S. C. Henderson, and D. J. Sutkus, Scheduled Civil Aircraft Emission Inventories Projected for 2015: Database Development and Analysis, *NASA CR-1998-207638,* 1998.

[5] CAEP/4-FESG/Report-4, Report of the Forecasting and Economic Analysis Sub-Group (FESG), *Long-Range Scenarios*, CAEP Steering Group Meeting, Canberra, January 1998.

[6] Fahey, D. W., et al., Emission measurements of the Concorde supersonic aircraft in the lower stratosphere, *Science, 270,* 70-74, 1995.

[7] Hagen, D., P. Whitefield, J. Paladino, M. Trueblood, and H. Lilenfeld, Particulate sizing and emission indices for a jet engine exhaust sampled at cruise, *Geophys. Res. Lett., 25,* 1681-1684, 1998.

[8] Miake-Lye, R. C., et al., SO_x oxidation and volatile aerosol in aircraft exhaust plumes depend on fuel sulfur content, *Geophys. Res. Lett., 25,* 1677-1680, 1998.

[9] Mortlock, A. M., and R. van Alstyne, Military, Charter, Unreported Domestic Traffic and General Aviation: 1976, 1984, 1992, and 2015 Emission Scenarios, *NASA CR-1998-207639,* 1998.

[10] Weisenstein, D. K., M. K. W. Ko, N-D Sze,and J. M. Rodriguez, Potential impact of SO_2 emissions from stratospheric aircraft on ozone, *Geophys. Res. Lett., 23,* 161-164, 1996.

[11] Weisenstein, D. K., G. K. Yue, M. K. W. Ko, N-D. Sze, J. M. Rodriguez, C. J. Scott , A two-dimensional model of sulfur species and aerosol, *J. Geophys. Res., 102,* 13,019-13,035, 1997.

[12] Weisenstein, D. K., M. K. W. Ko, I.G . Dyominov, G. Pitari, L. Ricciardulli, G. Visconti, and S. Bekki, The effect of sulfur emissions from HSCT aircraft: A 2-D model intercomparison, *J. Geophys. Res., 103,* 1527-1547, 1998.

[13] World Meteorological Organization (WMO), Scientific Assessment of Ozone Depletion: 1991, Global Ozone Res. and Monit. Proj., *Rep. 25,* Geneva, Switzerland, 1992.